JOC*Article*

Density Functional Theory Study of Electroreductive Hydrocoupling of α,β-Unsaturated Carbonyl Compounds

Naoki Kise

Department of Biotechnology, Faculty of Engineering, Tottori University, Koyama, Tottori 680-8552, Japan

kise@bio.tottori-u.ac.jp

Received August 17, 2006

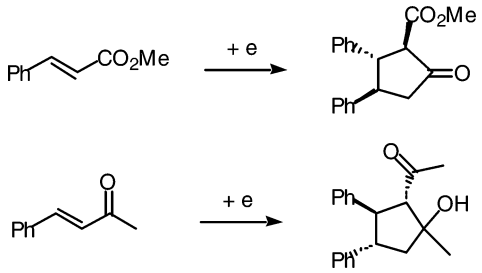

The electroreductive hydrocoupling of methyl cinnamate, methyl crotonate, cumarin, and benzalacetone was studied by DFT (B3LYP/6-311++G**) calculations. The computational outcomes for the transition states in the hydrocoupling of anion radicals generated by a one-electron transfer to the α,β-unsaturated carbonyl compounds well agree with the diastereoselectivities in the experimental results previously reported.

Introduction

Electroreductive hydrodimerization of acrylic acid derivatives is a well-known method for the synthesis of adipic acid derivatives.[1] Although this type of reaction is usually nondiastereoselective, several papers have reported that the electroreduction of cinnamic acid esters in aprotic solvents gave all-trans cyclized hydrodimers (*dl*-hydrodimers) stereospecifically.[2] This high dl selectivity has been explained by the interaction of anion radicals with the cathode surface[2a,b] or water.[3] Recently, we have reinvestigated the stereoselectivity of the electroreductive hydrocoupling of methyl cinnamate (**1**) in aprotic solvents and found that all-trans cyclized hydrodimer **2** was formed together with a small amount of the meso isomer of hydrodimer **3**.[4] Nevertheless, the dl selectivity of the hydrodimers is still high (58−90% diastereomeric excess (de)). On the other hand, the dl selectivity in the hydrodimer **5** derived from methyl crotonate (**4**) was low (34% de), and it is noted that the hydrocoupling of cumarin (**6**) brought about the corresponding hydrodimer **7** meso selectively in 50% de. In addition, we have reported that the electroreductive hydrocoupling of benzalacetone (**8**) also gave cyclic hydrodimer **9** and a

(1) (a) Baizer, M. M. *J. Electrochem. Soc.* **1964**, *111*, 215−222. (b) Baizer, M. M.; Anderson, J. D. *J. Electrochem. Soc.* **1964**, *111*, 223−226. (c) Rifi, M. R. In *Technique of Electroorganic Synthesis, Part II*; Weinberg, N. L., Ed.; Wiley: New York, 1975; pp 192−215.

(2) (a) Klemm, L. H.; Olson, D. R. *J. Org. Chem.* **1973**, *58*, 3390−3394. (b) Kanetsuna, H.; Nonaka, T. *Denki Kagaku* **1981**, *49*, 526−531. (c) Smith, C. Z.; Utley, H. P. *J. Chem. Soc., Chem. Commun.* **1981**, 492−494. (d) Nishiguchi, I.; Hirashima, T. *Angew. Chem., Int. Ed. Engl.* **1983**, *22*, 52−53. (e) Utley, J. H. P.; Güllü, M.; Motevalli, M. *J. Chem. Soc., Perkin Trans. 1* **1995**, 1961−1970.

(3) Fussing, I.; Güllü, M.; Hammerich, O.; Hussain, A.; Nielsen, M. F.; Utley, J. H. P. *J. Chem. Soc., Perkin Trans. 2* **1996**, 649−658.

(4) Kise, N.; Iitaka, S.; Iwasaki, K.; Ueda, N. *J. Org. Chem.* **2002**, *67*, 8305−8315.

(5) Kise, N.; Kitagishi, Y.; Ueda, N. *J. Org. Chem.* **2004**, *69*, 959−963.

(6) Recent reports containing the DFT calculations of transition states to elucidate the diastereoselectivity in a carbon−carbon bond formation, see: (a) Gordillo, R.; Houk, K. N. *J. Am. Chem. Soc.* **2006**, *128*, 3543−3553. (b) Ando, K. *J. Org. Chem.* **2006**, *71*, 1837−1850. (c) Iafe, R. G.; Houk, K. N. *Org. Lett.* **2006**, *8*, 3469−3472. (d) Aggarwal, V. K.; Charmant, J. P. H.; Fuentes, D.; Harvey, J. N.; Hynd, G.; Ohara, D.; Picoul, W.; Robiette, R.; Smith, C.; Vasse, J.-L.; Winn, C. L. *J. Am. Chem. Soc.* **2006**, *128*, 2105−2114. (e) Afarinkia, K.; Bahar, A.; Bearpark, M. J.; Garcia-Ramos, Y.; Ruggiero, A.; Neuss, J.; Vyas, M. *J. Org. Chem.* **2005**, *70*, 9529−9537. (f) Clemente, F. R.; Houk, K. N. *J. Am. Chem. Soc.* **2005**, *127*, 11294−11302. (g) Rulisek, L.; Sebek, P.; Havlas, Z.; Hrabal, R.; Capek, P.; Svatos, A. *J. Org. Chem.* **2005**, *70*, 6295−6302. (h) Bassan, A.; Zou, W.; Reyes, E.; Himo, F.; Cordova, A. *Angew. Chem., Int. Ed.* **2005**, *44*, 7028−7032. (i) Paddon-Row, M. N.; Moran, D.; Jones, G. A.; Sherburn, M. S. *J. Org. Chem.* **2005**, *70*, 10841−10853. (j) Bakalova, S. M.; Santos, A. G. *J. Org. Chem.* **2004**, *69*, 8475−8481. (k) Cheong, P. H.-Y.; Houk, K. *J. Am. Chem. Soc.* **2004**, *126*, 13912−13913. (l) Macias, A.; Alonso, E.; del Pozo, C.; Venturini, A.; Gonzalez, J. *J. Org. Chem.* **2004**, *69*, 7004−7012. (m) Kise, N. *J. Org. Chem.* **2004**, *69*, 2147−2152.

10.1021/jo061708k CCC: $33.50
Published on Web 10/25/2006

SCHEME 1

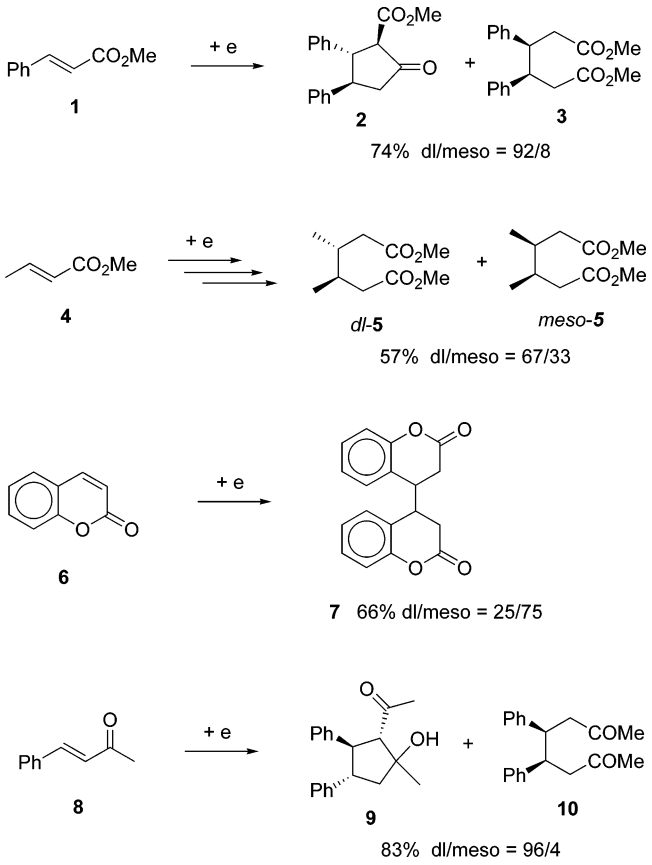

small amount of hydrodimer **10** with high dl diastereoselectivity.[5] We have already calculated the transition states for the electroreductive hydrodimerization of methyl cinnamate, cumarin, and benzalacetone with semi-empirical methods to explain the diastereoselectivity.[4,5] In this paper, we recalculated the transition states for these electroreductive hydrocouplings (Scheme 1) more precisely with DFT methods at the B3LYP/6-311++G** level to elucidate the diastereoselectivity without supposing intuitive interactions.[6] The calculation results well explain the diastereoselectivities, in particular, the high dl selectivity in the hydrocoupling of **1** and **8**.

Results and Discussion

(1) Calculations for Radical Anions Generated from 1, 4, 6, and 8. The reaction mechanism of the electroreductive hydrocoupling of **1** in aprotic solvents has been discussed previously.[4,7] It has been recognized that the radical anions generated by a one-electron transfer to **1** couple with each other, and then the resulting hydrodimer cyclizes to all-trans **2** (Scheme 2). We therefore calculated spin and charge densities of the radical anions (RA) generated from **1**, **4**, **6**, and **8** by the DFT method at the B3LYP/6-311++G** level (Table 1). In all cases, the carbons β to the carbonyl group have the highest spin density as well as a low positive or negative charge density (indicated by boldface in Table 1). These results also support that the electroreductive hydrocoupling of **1**, **4**, **6**, and **8** proceeds through homocoupling at the carbons β to the carbonyl group in the radical anions.

(7) Hammerich, O.; Nielsen, M. F. *Acta Chem. Scand.* **1998**, *52*, 831−857.

SCHEME 2

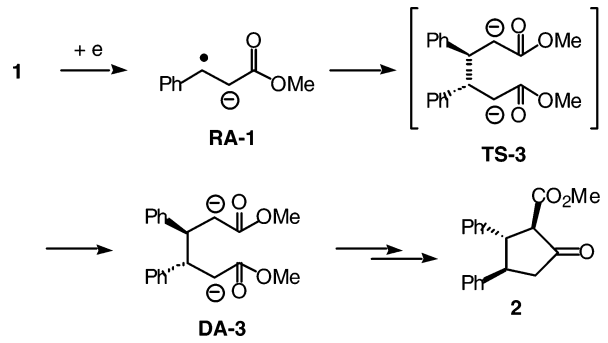

(2) Calculations for Transition States in Electroreductive Hydrocoupling of Methyl Cinnamate (1). We carried out DFT calculations of the transition states for the homocoupling of the radical anion derived from **1**. The geometry optimizations were carried out at the B3LYP/6-311++G** level. The optimized structures of the transition states (TS) leading to *dl*- and *meso*-hydrodimers **3** are shown in Figure 1. The relative energies of the optimized transition states of **TS-3** for the dimerization of **RA-1** and dl/meso ratios calculated from the relative energies of the transition states are summarized in Table 2. Single point calculations by the MP2/6-311++G** method were also performed. The results of the calculations nicely support the high dl selectivity in the hydrocoupling of **1**, although the calculated dl/meso ratios are somewhat higher than that in the experimental result (dl/meso = 92/8). These computational results suggest that the high dl selectivity can be explained without assuming unusual interactions between the radical anions and the cathode surface[2a,b] or water.[3] These intuitive interactions seem to be proposed necessarily from the common reason that the *meso*-hydrodimer is thermodynamically more stable than the *dl*-hydrodimer. To ascertain if the reason is valid in this case, we carried out DFT calculations for the dianions (DA) of the hydrodimers **3**. The optimized structures and their relative energies of ***dl*-** and ***meso*-DA-3** are illustrated in Figure 2. These results imply that *dl*-dianion is more stable than *meso*-dianion in CH_3CN whereas the relative stability changes inversely in the gas phase. Therefore, the common reason may be a fixed idea that does not always apply. In addition, the calculations disclose that the solvation with CH_3CN strongly lowers the activation energies for the dimerization of **RA-1** (Table 2).

(3) Calculations for Transition States in Electroreductive Hydrocoupling of Methyl Crotonate (4). Next, the electroreductive hydrocoupling of **4** was studied by the B3LYP/6-311++G** method. The optimized structures of **TS-5** for the dimerization of **RA-4** and their relative energies are depicted in Figure 3 and Table 3. The calculated dl/meso ratio in the gas phase closely agrees with that in the experimental result (dl/meso = 67/33), while the dl selectivity calculated using the polarizable continuum models (PCM) for the CH_3CN solvent is too high. More or less, the calculations support the dl selectivity in the hydrocoupling of **4**.

(4) Calculations for Transition States in Electroreductive Hydrocoupling of Cumarin (6). We have reported that the electroreductive hydrocoupling of **6** gave the dimer **7** in a 25/75 diastereomeric ratio of dl/meso. In the preliminary report,[4] the stereoconfiguration of **7** was assigned by transformation to its analogue of **3**. In this study, we directly confirmed the

TABLE 1. Spin and Charge Densities of Radical Anions of 1, 4, 6, and 8 Calculated by the UB3LYP/6-311++G Method[a]**

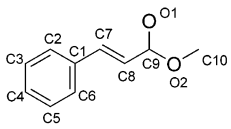

RA-1

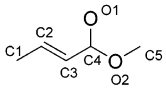

RA-4

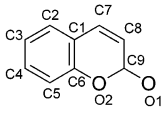

RA-6

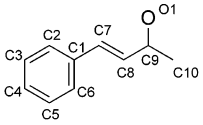

RA-8

	RA-1		RA-4		RA-6		RA-8	
	spin[b]	charge[c]	spin[b]	charge[c]	spin[b]	charge[c]	spin[b]	charge[c]
C1	0.01	0.36	-0.44	0.11	-0.07	0.24	-0.06	0.46
C2	0.15	-0.28	**0.79**	**-0.21**	0.23	-0.25	0.14	-0.30
C3	-0.04	0.22	-0.03	-0.69	-0.09	0.05	-0.04	0.22
C4	0.25	-0.50	0.25	1.62	0.23	-0.39	0.23	-0.49
C5	-0.07	0.23	-0.05	0.38	-0.02	0.17	-0.07	0.22
C6	0.17	-0.28			0.06	0.19	0.17	-0.28
C7	**0.26**	**0.06**			**0.28**	**-0.02**	**0.27**	**-0.11**
C8	0.16	-0.82			0.24	-0.43	0.08	-0.66
C9	0.07	1.88			0.07	1.22	0.12	1.18
C10	0.00	0.42					-0.01	-0.17
O1	0.09	-1.09	0.11	-1.11	0.09	-1.17	0.15	-1.08
O2	0.01	-1.20	0.02	-1.10	0.04	-0.61		

[a] The values in boldface are of the carbons β to the carbonyl group. [b] Mulliken spin densities. [c] APT atomic charges with hydrogens summed into heavy atoms.

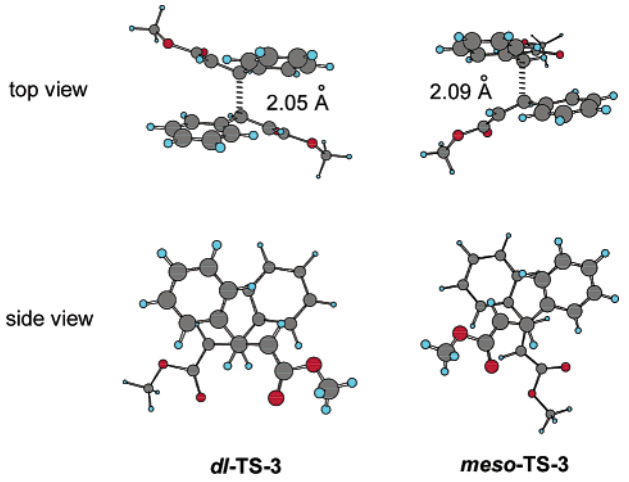

FIGURE 1. Optimized structures of transition states for the hydrocoupling of **1**.

stereostructure of the minor isomer of **7** to be dl by means of X-ray crystallographic analysis (Supporting Information).

The calculations for the transition states **TS-7** in the dimerization of **RA-6** were carried out by the B3LYP/6-311++G** method. The results of optimization are exhibited in Figure 4 and Table 4. The calculated meso selectivity using the PCM models for the CH_3CN solvent is slightly higher than that in the experimental result (dl/meso = 25/75), whereas from the calculations in the gas phase, the meso selectivity is evaluated to be considerably high. It can be pointed out that these results well accord with the meso selectivity in the hydrocoupling of **6**.

(5) Calculations for Transition States and Cyclic Dimer Anions in Electroreductive Hydrocoupling of Benzalacetone (8). Finally, the electroreductive hydrocoupling of **8** was studied by the B3LYP/6-311++G** method. The optimized structures of **TS-10** for the dimerization of **RA-8** are shown in Figure 5, and their relative energies are summarized in Table 5. The calculated dl/meso ratio in the gas phase is very consistent with that in the experimental result (dl/meso = 96/4), while the calculations using the PCM models for the CH_3CN solvent overestimate the dl selectivity. At any rate, the results of calculations nicely explain the high dl selectivity in the hydrocoupling of **8**.

In the preliminary report,[5] we reported that the dl hydrodimer was obtained as a diastereomeric mixture of two cyclized dimmers, **9a**,**b** (**9a**/**9b** = 58/42), of four possible diastereomers, **9a**−**d**, and that the formation of **9** was determined by equilibrium between diastereomers of the cyclized *O*-anion (CA) of **9** (Scheme 3). Thus, DFT calculations for the four possible stereoisomers of **CA-9** were performed at the B3LYP/6-311++G** level with the PCM model for the CH_3CN solvent to evaluate their thermodynamic stability more precisely (Figure 6). These computational results are in accordance with the formation of **9a**,**b**. Namely, the two isomers, **CA-9a** and **CA-9b**, are much more stable (>2.84 kcal/mol) than the other two isomers, **CA-9c** and **CA-9d**, although **CA-9b** is somewhat more stable (0.44 kcal/mol) than **CA-9a**.

Conclusion

The electroreductive hydrocoupling of methyl cinnamate, methyl crotonate, cumarin, and benzalacetone was computationally studied with the DFT method at the B3LYP/6-311++G** level to explain the diastereoselectivities experimentally observed in the electroreduction of these α,β-unsaturated carbonyl compounds. The structures of the transition states leading to the *dl*- and *meso*-hydrodimers were optimized, and their relative energies were converted to the dl/meso ratios of the hydrodimers to compare with the diastereomeric ratios in the experimental results. It is concluded that the calculation results well explain the high dl selectivity in the hydrocoupling of methyl cinnamate and benzalacetone, the moderate dl selectivity in the hydrocoupling of methyl crotonate, and the meso selectivity in the hydrocoupling of cumarin. It is also

TABLE 2. Relative Energies (kcal/mol) of Transition States Optimized by the B3LYP/6-311++G Method and dl/meso Ratios for Hydrocoupling of 1**

	B3LYP/6-311++G**				MP2/6-311++G**[e]		
	gas[a]	gas[a,b]	PCM[a,c]	CPCM[a,d]	gas[a]	PCM[a,c]	exptl[f]
***dl*-TS-3**	0 (68.10)	0 (82.88)	0 (17.05)	0 (16.85)	0 (96.37)	0 (49.09)	
***meso*-TS-3**	2.27 (70.37)	1.82 (84.70)	2.33 (19.38)	2.31 (19.17)	2.25 (98.61)	1.99 (51.09)	
dl/meso	98/2	96/4	98/2	98/2	98/2	97/3	92/8

[a] The values in parentheses are energies (kcal/mol) presented with **RA-1** as reference. [b] Thermally corrected to 298 K. [c] Using the IEFPCM model for the CH_3CN solvent. [d] Using the CPCM model for the CH_3CN solvent. [e] Single point calculation. [f] Experimental data.

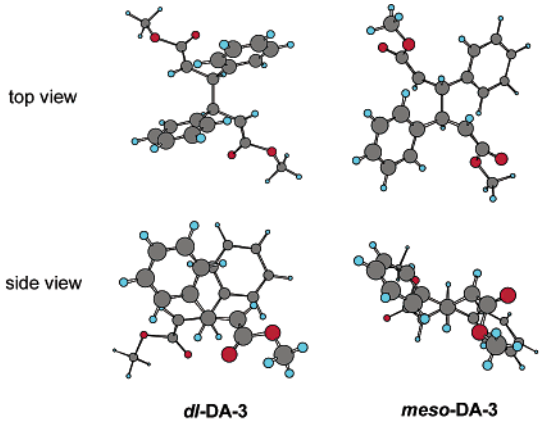

	gas	gas[a]	PCM[b]	CPCM[c]
***dl*-DA-3**	0	2.16	0	0
***meso*-DA-3**	0.26	0	3.51	3.55

[a]Thermally corrected to 298 K. [b]Using the IEFPCM model for CH_3CN solvent. [c]Using the CPCM model for CH_3CN solvent.

FIGURE 2. Optimized structures and relative energies of dianions of **3**.

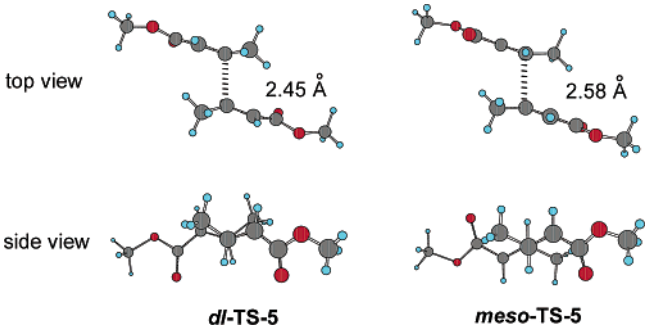

FIGURE 3. Optimized structures of transition states for the hydrocoupling of **4**.

disclosed that the solvation with CH_3CN strongly lowers the activation energies for the dimerization of radical anions. In addition, the thermodynamic formation of the two isomers of the cyclized dimer in the hydrocoupling of benzalacetone is supported by the calculations of the four possible isomers of the cyclized dimer *O*-anion.

Experimental Section

Computational Methodology. All calculations were carried out with the Gaussian 03 program.[8] Geometry optimization was performed by the B3LYP/6-311++G** method throughout. All optimized geometries were verified by the vibrational analysis, and their energies were thermally corrected to 298 K based on the frequencies. As for the transition states, it was confirmed that these structures had only one imaginary frequency. The imaginary frequency was ascertained to be consistent with the hydrocoupling by displaying the vibrational mode using the Gauss View program. In addition, single-point calculations were carried out for all optimized transition states using the PCM calculations with the integral equation formalism model (IEFPCM) and polarizable

TABLE 3. Relative Energies (kcal/mol) of Transition States Calculated by the B3LYP/6-311++G Method and dl/meso Ratios for Hydrocoupling of 4**

	gas	gas[a]	PCM[b]	CPCM[c]	exptl[d]
***dl*-TS-5**	0	0	0	0	
***meso*-TS-5**	0.42	0.20	3.38	3.44	
dl/meso	67/33	58/42	>99/1	>99/1	67/33

[a] Thermally corrected to 298 K. [b] Using the IEFPCM model for CH_3CN solvent. [c] Using the CPCM model for CH_3CN solvent. [d] Experimental data.

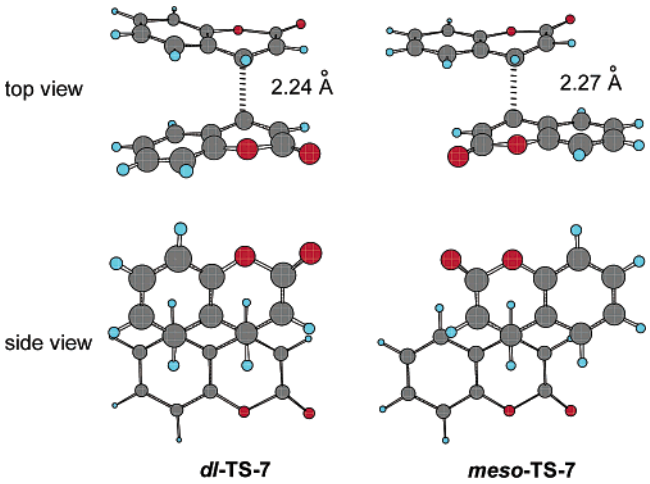

FIGURE 4. Optimized structures of transition states for the hydrocoupling of **6**.

(8) The calculations were carried out using the Gaussian 03 program. Frisch, M. J.; Trucks, G. W.; Schlegel, H. B.; Scuseria, G. E.; Robb, M. A.; Cheeseman, J. R.; Montgomery, J. A., Jr.; Vreven, T.; Kudin, K. N.; Burant, J. C.; Millam, J. M.; Iyengar, S. S.; Tomasi, J.; Barone, V.; Mennucci, B.; Cossi, M.; Scalmani, G.; Rega, N.; Petersson, G. A.; Nakatsuji, H.; Hada, M.; Ehara, M.; Toyota, K.; Fukuda, R.; Hasegawa, J.; Ishida, M.; Nakajima, T.; Honda, Y.; Kitao, O.; Nakai, H.; Klene, M.; Li, X.; Knox, J. E.; Hratchian, H. P.; Cross, J. B.; Bakken, V.; Adamo, C.; Jaramillo, J.; Gomperts, R.; Stratmann, R. E.; Yazyev, O.; Austin, A. J.; Cammi, R.; Pomelli, C.; Ochterski, J. W.; Ayala, P. Y.; Morokuma, K.; Voth, G. A.; Salvador, P.; Dannenberg, J. J.; Zakrzewski, V. G.; Dapprich, S.; Daniels, A. D.; Strain, M. C.; Farkas, O.; Malick, D. K.; Rabuck, A. D.; Raghavachari, K.; Foresman, J. B.; Ortiz, J. V.; Cui, Q.; Baboul, A. G.; Clifford, S.; Cioslowski, J.; Stefanov, B. B.; Liu, G.; Liashenko, A.; Piskorz, P.; Komaromi, I.; Martin, R. L.; Fox, D. J.; Keith, T.; Al-Laham, M. A.; Peng, C. Y.; Nanayakkara, A.; Challacombe, M.; Gill, P. M. W.; Johnson, B.; Chen, W.; Wong, M. W.; Gonzalez, C.; Pople, J. A. *Gaussian 03*, revision C.02; Gaussian, Inc.: Wallingford, CT, 2004.

TABLE 4. Relative Energies (kcal/mol) of Transition States Calculated by the B3LYP/6-311++G Method and dl/meso Ratios for Hydrocoupling of 6**

	gas	gas[a]	PCM[b]	CPCM[c]	exptl[d]
***dl*-TS-7**	2.25	2.94	1.08	1.06	
***meso*-TS-7**	0	0	0	0	
dl/meso	2/98	1/99	14/86	14/86	25/75

[a] Thermally corrected to 298 K. [b] Using the IEFPCM model for CH_3CN solvent. [c] Using the CPCM model for CH_3CN solvent. [d] Experimental data.

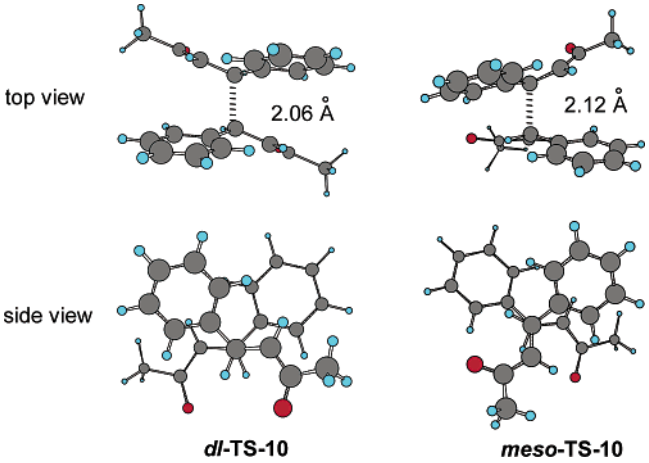

FIGURE 5. Optimized structures of transition states for the hydrocoupling of **8**.

TABLE 5. Relative Energies (kcal/mol) of Transition States Calculated by the B3LYP/6-311++G Method and dl/meso Ratios for Hydrocoupling of 8**

	gas	gas[a]	PCM[b]	CPCM[c]	exptl[d]
***dl*-TS-10**	0	0	0	0	
***meso*-TS-10**	1.24	1.51	4.27	4.31	
dl/meso	89/11	93/7	>99/1	>99/1	96/4

[a] Thermally corrected to 298 K. [b] Using the IEFPCM model for CH_3CN solvent. [c] Using the CPCM model for CH_3CN solvent. [d] Experimental data.

conductor calculation models (CPCM) for CH_3CN solvent at the same level as the geometry optimization (B3LYP/6-311++G**) to take the solvent effect into consideration. For the structures of **TS-3**, single-point calculations with the MP2/6-311++G** method were also performed with and without using IEFPCM (CH_3CN). The optimization of **CA-9** was carried out using the IEFPCM model for CH_3CN solvent at the B3LYP/6-311++G** level.

X-ray Crystallographic Analysis of *dl*-7. All measurements were made on a Rigaku RAXIS imaging plate area detector with graphite monochromated Mo Kα radiation. The structure was solved by direct methods with SIR92 and expanded using Fourier techniques with DIRDIF99. The non-hydrogen atoms were refined anisotropically. Hydrogen atoms were refined isotropically. All calculations were performed using the CrystalStructure crystallographic software package.

Supporting Information Available: Data for all of the calculated radical anions, transition states, and cyclic anions **CA-9**, as well as X-ray crystallographic structure (ORTEP) of ***dl*-7**, and a crystallographic cif file for ***dl*-7**. This material is available free of charge via the Internet at http;//pubs.acs.org.

JO061708K

SCHEME 3

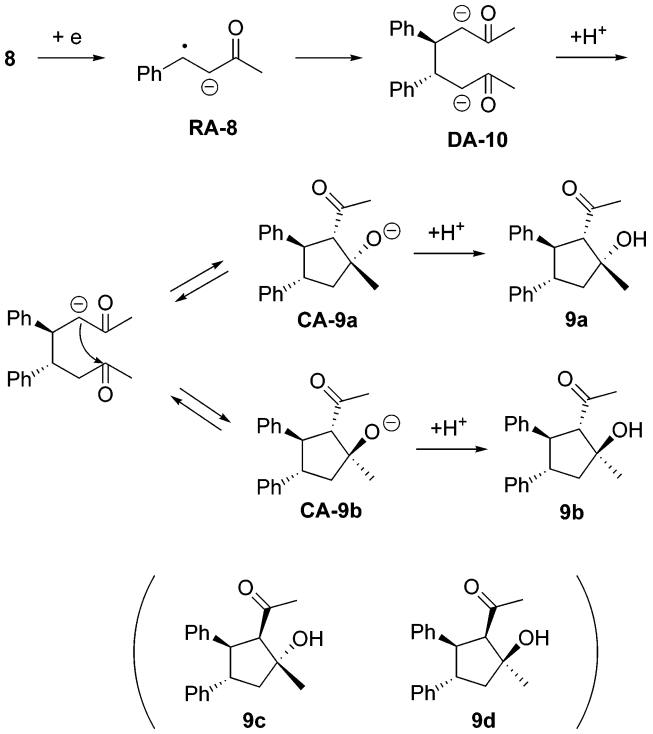

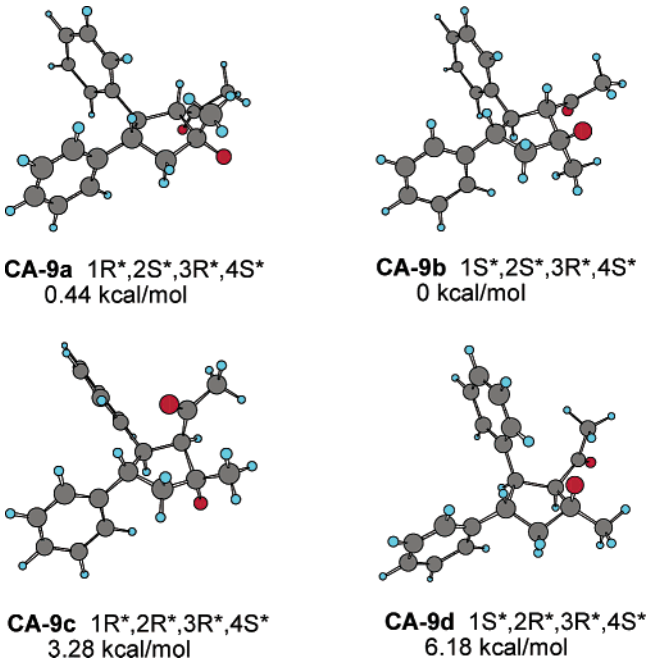

FIGURE 6. Optimized structures and relative free energies of four isomers of **CA-9**.